

## Survey of AZ31/HA-Zeolite Nano Crystalline Biocomposite with Powder Metallurgy (PM)

Mehrdad Soltani<sup>1\*</sup>, Ebrahim Karamian<sup>2</sup>, Majid Karimian<sup>3</sup>

<sup>1,3</sup>Department of Mechanical Engineering, Khominishahr Branch, Islamic Azad University, Iran

<sup>2</sup>Advanced Materials Research Center, Faculty of Materials Engineering, Najafabad Branch, Islamic Azad University, Najafabad, Iran

\*Email of corresponding author: Mehrdad.Soltani@ymail.com

Received: January 5, 2016; Accepted: April 14, 2016

### Abstract

Magnesium is potentially useful for orthopedic and cardiovascular applications. Magnesium and its alloys are light, biodegradable, biocompatible metals that have promising applications as biomaterials. However, the corrosion rate of this metal is so high that its degradation occurs before the end of the healing process. One of the ways to improve the corrosion rate is to compose it with ceramic materials such as HA, TCP and so on. In this study, at first, the alloy with a nominal composition of Mg-3%Al-1%Zn (AZ31 alloy) was produced by high energy ball milling (HEBM) of Mg powder, Zn powder and Al powder under high purity argon. The ball milling parameters were chosen as following: shaft rotation was 600 rpm, ratio of balls to powder was 10:1 and milling time was 90, 180, 270 and 360 min under argon atmosphere. The obtained Mg alloy powders were pressed with different amounts of HA-Zeolite (HZ) powder mixture, weight ratio HA (Hydroxyapatite) to Zeolite 4:1, under 1000 MPa in steel die with 12 mm in diameter and 20 mm in height. The pressed samples were sintered for 1 h at 630 K in an inert atmosphere furnace. Microstructure characterization of as-milled powders and as-sintered alloys were carried out by SEM. An X-ray diffraction (XRD) was used for phase analysis. XRD patterns of the powders mixture showed that the AZ31 alloy powder has been gained after 270 min.

### Keywords

AZ31, HA-Zeolite, Mechanical Alloying, Powder Metallurgy, Bio Composite

### 1. Introduction

During the last decade, nanocrystalline and ultra-fine-grained materials have received considerable attention. These materials improved mechanical properties as compared with conventional coarse-grained materials [1-4]. For example, when the grain size was reduced to about 0.5 micron, Mg alloy showed a yield stress of 410 MPa with a 12% elongation. In addition, because of Mg alloys, there was widespread attention as new biodegradable orthopedics materials due to low density, suitable method properties in heat [1-5]. The powder metallurgy technique (PM) requires a low cost energy and gains uniformity in reinforcement distribution, which is difficult to be obtained by conventional casting methods [6]. Combination of PM and mechanical alloying, MA, with severe plastic deformation (SPD) techniques such as equal angular pressing and high ratio extrusion improve the uniformity of the reinforcement particle distribution in nanocomposites [7]. The fabrication of in situ nanocomposite-like microstructures in an AZ61 Mg alloy using ingot process method was reported by Avedisian et al in 2002. The equilibrium volume fraction of B-Mg<sub>17</sub>Al<sub>12</sub> intermetallic phase in AZ61 is approximately 6% at room temperature.

The B phase is practically under formable at ambient temperatures because it becomes soft and plastically deformable above 150°C. So, B-Mg<sub>17</sub>Al<sub>12</sub> can effectively reinforce AZ61 when its size is very small and its distribution is uniform, although AZ61 is not usually classified as a composite. This composite showed a suitable cytocompatible, mechanical and corrosion properties [8-14]. Lizi et al indicated that Mg-Ca alloys have appropriate mechanical properties and good biocompatibility. Mechanical alloying, (MA), is one of the most cost-effective processes that have proven to be capable of producing powders with nano-sized structure [15-16]. This method has been utilized in fabrication of different products such as nano-crystalline alloys, intermetallic compounds and metal matrix composites [17-19]. Moreover, there is limited information reported on the fabrication of nano-crystalline ternary titanium alloy systems such as Ti-Al-v, Ti-Al-Si and Ti-Al-Mg, by MA process [20]. In this study, the mechanical alloying process, (MA), was employed to prepare AZ31 alloys and the PM technique was applied to compact AZ31/HA-Zeolite composite. This biocomposite contains low Al element, neuro-toxicant element for biological human system, and high Mg. The aim of this work is to fabricate AZ31/HA-Zeolite composite nanobiocomposite to use orthopedic applications.

## 2. Materials and method

The alloy with a nominal composition of Mg-3%Al-1%Zn (AZ31 alloy) was produced by high energy ball milling (HEBM) of Mg powder (99%, 270Mesh), Zn powder (99%, 270 Mesh) and Al powder (99.5%, 270 Mesh) under high purity argon(99.9%). The ball milling was performed with F124 planetary ball milling machine and balls were stainless steel. The ball milling parameters were chosen as following: shaft rotation was 600 rpm, ratio of balls to powder was 10:1 and milling time was 90,180,270 and360 min. The vial of stainless steel was filled with high purity argon, so the milling process was carried out under an inert atmosphere. The obtained Mg alloy powders were pressed with different amounts of HA-Zeolite (HZ) powder mixture, weight ratio HA (Hydroxyapatite) to Zeolite 4:1, under 1000 MPa in steel die with 12 mm in diameter and 20 mm in height. The pressed samples were sintered for 1h at 630K in an inert atmosphere furnace. Mechanical strength and elongation (EL. %) of sintered samples were performed based on ASTM 1022 and 1024 with an INSTURN machine with an initial strain ratio of 0.001sec. Hardness of the samples was carried out by Vickers method. Microstructure characterization of as-milled powders and as-sintered alloys were carried out by SEM. X-ray phase analysis was performed with Zaies 11004 machine, using Cu K<sub>α</sub> radiation.

## 3. Results and Discussion

### 3.1 XRD results

Figure 1 shows XRD patterns of the metal powders mixture milled for 0, 90, 180, 270 and 360 min. Figure 2 shows XRD patterns of the powders mixture milled at 36.6° approximately position. As it can be seen in this figure, the strongest Mg peak lightly shifted to right direction in the samples milled for 270 and 360 min. It means that Al and Zn elements doped in Mg crystal structure and the AZ31 alloy powder has been gained after 270 min. Regarding to atomic reduces of Mg, Zn and Al, 0.145, 0.142 and 0.118 nm, respectively, it can be concluded that with substitution of Al and Zn atoms instead of Mg atom in Mg crystal structure, lattice parameter or distance crystalline planes will be decrease. According to Bragg's law,  $n\lambda=2d\sin\Theta$ , by increasing of distance crystalline planes,  $d$ ,  $\sin\theta$  will be decrease.

### 3.2 Crystalline size and lattice strain

Following graph is showing  $\beta \cos\theta$  versus  $\sin\theta$  for the sample milled for 270 min, MP270, according to XRD data in Figure 3 and 4. As mentioned at introduction section, crystallite size D

could be determined from the intersection of Williamson-Hall line at  $\sin\theta = 0$ . Also, lattice strain,  $\theta$ , could be calculated from the slope of Williamson-hall line. So, crystalline size,  $D$  and lattice strain of the sample, MP270, are calculated 47 nm and 0.03 %, respectively.

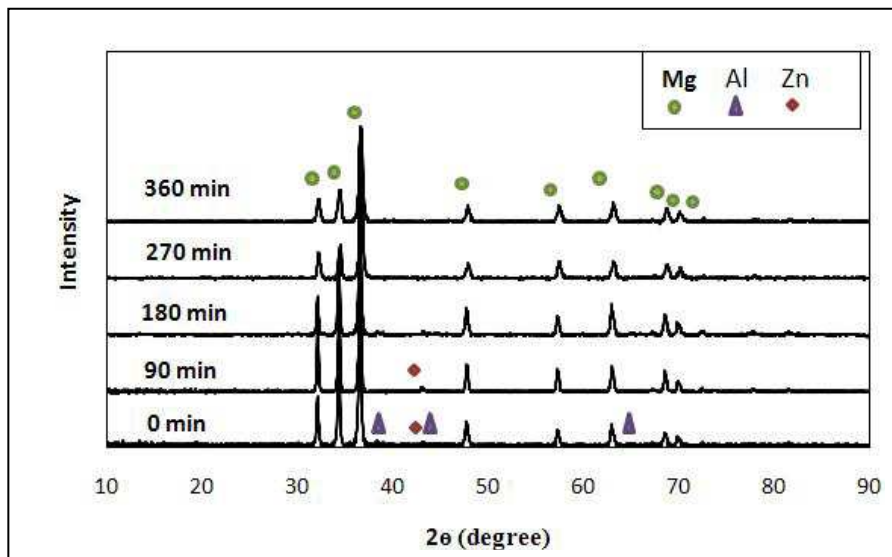


Figure1. XRD patterns of the metal powder mixture milled for 0, 180, 90, 270 and 360 min

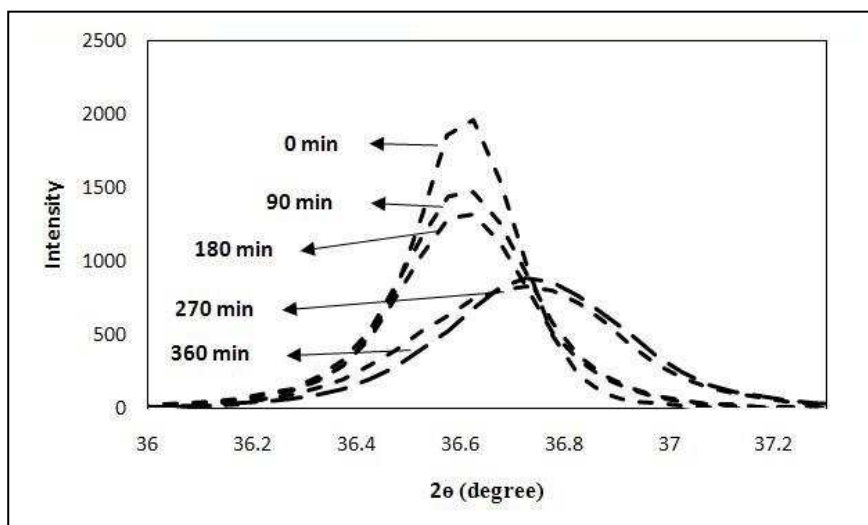


Figure2. XRD patterns of the metal powder mixture milled for 0, 180, 90, 270 and 360 min at the strongest peak

XRD patterns of the powders mixture milled for 270 and 360 min showed that the strongest Mg peak lightly shifted to right direction. It means that Al and Zn elements doped in Mg crystal structure and the AZ31 alloy powder has been gained after 270 min.

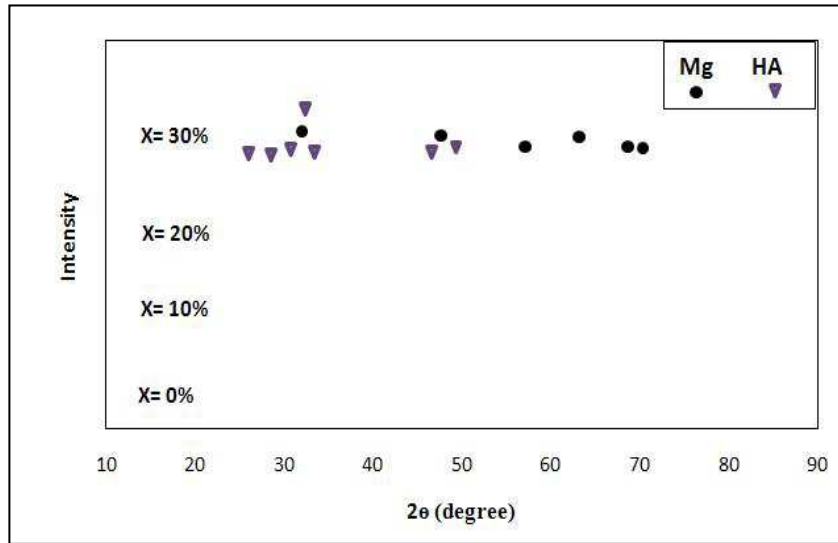


Figure3. XRD patterns of the metal and ceramic powders mixture compacted and sintered at 1300 °C for 1 h under argon inert atmosphere

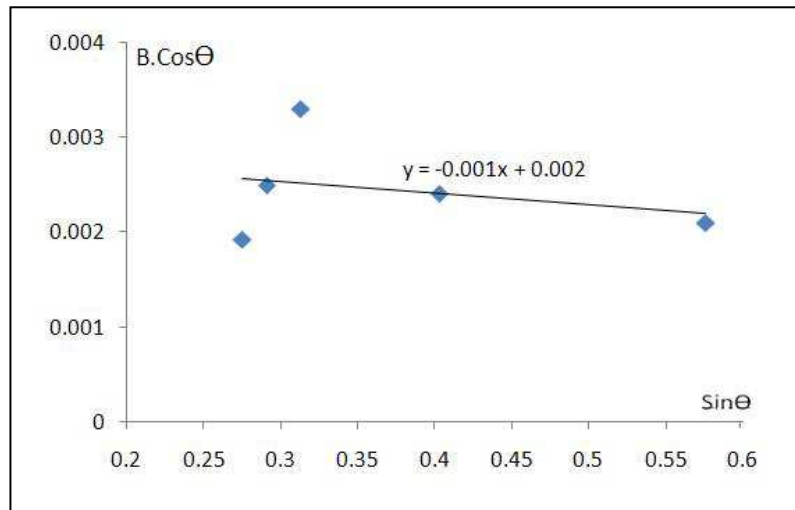


Figure4.  $\beta \cdot \cos\theta$  versus  $\sin\theta$  for the powder sample milled for 270 min

### 3.3 SEM micrographs

Figure 5 Shows SEM micrograph of metals powder morphology. As it can be seen, particles morphology Al, Zn and Mg are lately sphere and needle, respectively. Figure 6 shows the morphology of metal particles mixture after different milling time. As it has seen, by increasing milling time, the particle morphology has been spherical and round.

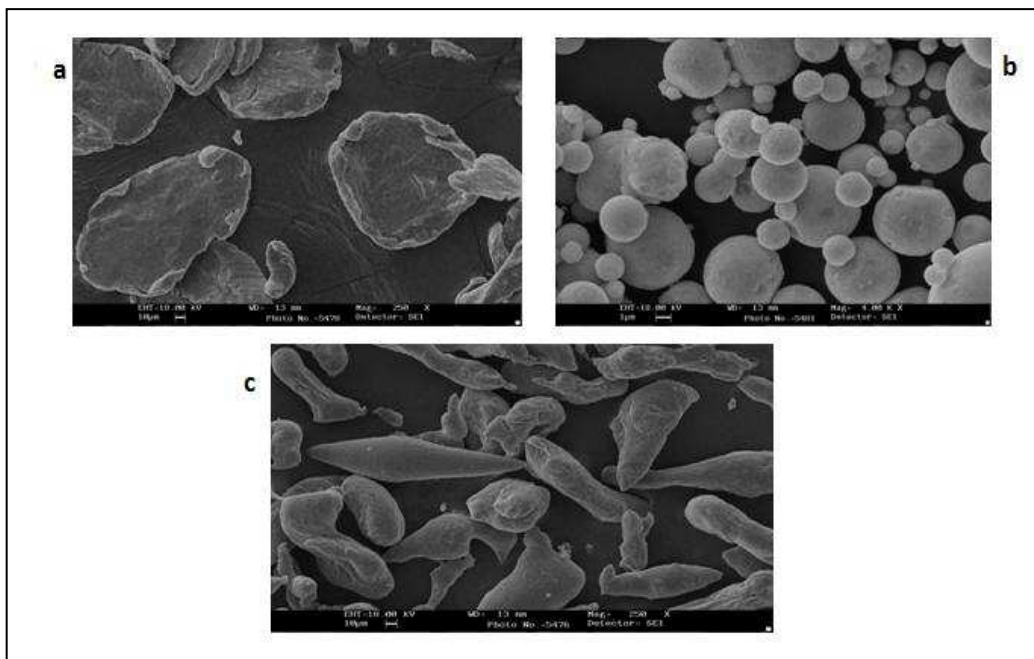


Figure5. SEM micrograph of metal powder morphology (a) Al, (b) Zn and (c) Mg before milling

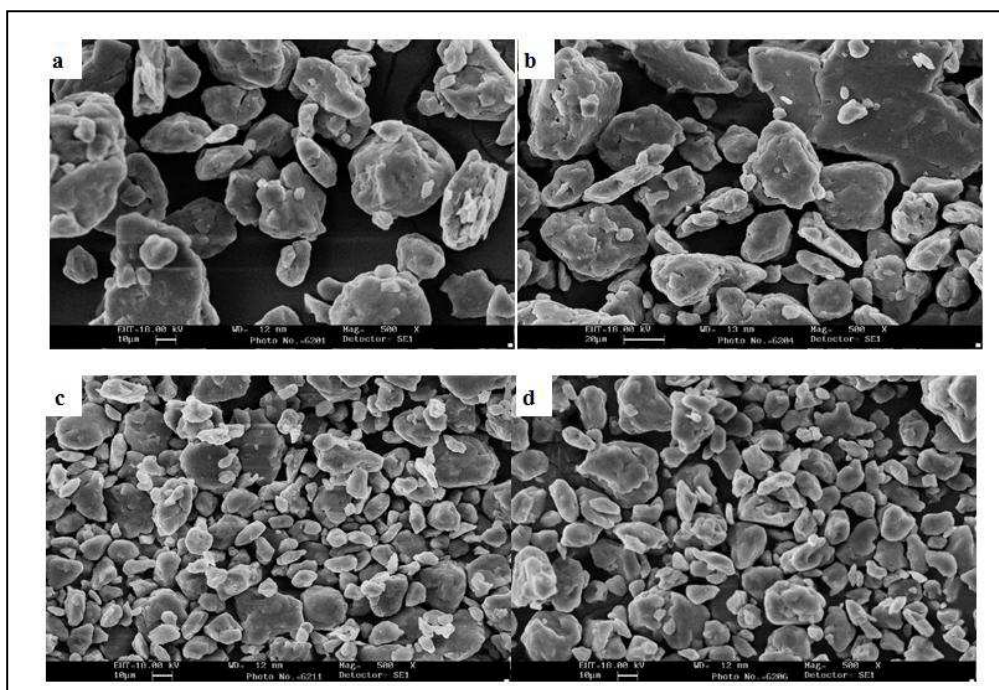


Figure6. SEM micrograph of metal powder mixture mechanically milled for (a) 90 min, (b) 180 min, (c) 270 min and (d) 360 min

#### 4. Mechanical Properties Results

##### 4.1 Strength and Elongation values

CCS and elongation (El. %) values of the samples are shown in the Figure 7. As it has seen in this figure, mechanical properties (CCS and elongation (El. %) values) have been improved by increasing weight percent of HZ mixture in the AZ31/HA-Zeolite composite samples. As shown in the Figure 7, by increasing ceramic phase, HZ mixture, in the composite samples CCS values

(mechanical strength)has been increased It seems that due to presence of ceramic phases between metal particles, the HZ mixture increases the metal particles sinter and finally improves the mechanical strength of the composite samples. In fact, presence of ceramic particles has acted as a sinter agent.

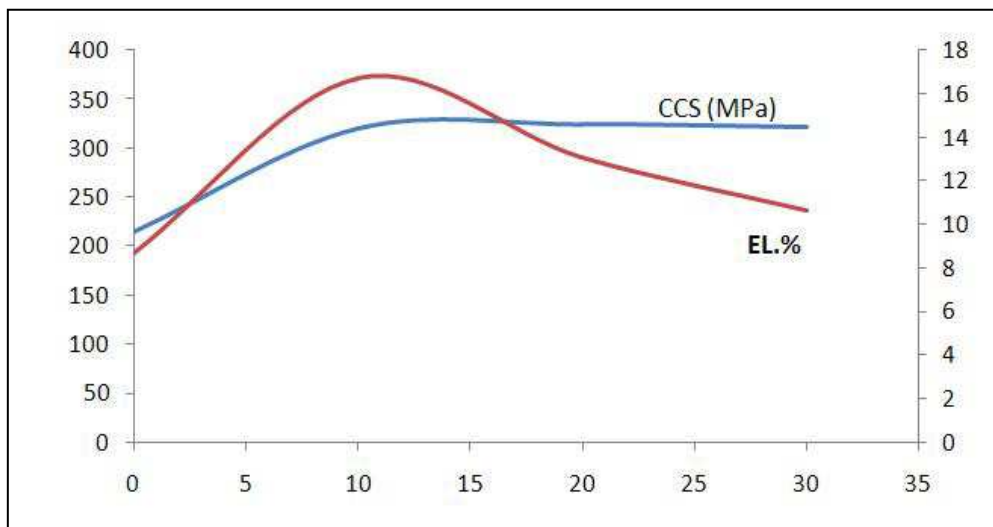


Figure7. CCS and elongation (El. %) values of the composite samples

### 5. Conclusion

According above discussion, we can conclude the following conclusions:

- 1- Al and Zn elements have been doped in Mg crystal structure and the AZ31 alloy powder has been gained after 270 min.
- 2-Crystalline size (D) and lattice strain ( $\theta$ ) of the sample milled for 270 are 47 nm and 0.03 %, respectively.
- 3- By increasing milling time, the particles morphology has been spheral and round.
- 4-Mechanical properties (CCS and elongation (El. %) values) have been improve by increasing weight percent of HA-Zeolite materials in the AZ31/HA-Zeolite composite samples.

### 6. References

- [1] Avedisian, M.M. and Baker, H. 2002. Magnesium and Magnesium Alloys, ASM Specially Handbook, 16-24.
- [2] Kim, W.J., Park, I.B. and Han, S.H. 2012. Formation of a nanocomposite-like microstructure in Mg-6Al-1Zn alloy, Scriptamaterialia, 66, 590-593.
- [3] Witte, et al. 2007. Biodegradable Mg-Hydroxyapatite metal matrix composite, biomaterials, 28, 2163-74.
- [4] Li, Z.j., Gu, X.N., Lou, S.Q. and Zheng, Y.F. 2008. The development of binary Mg-Ca alloys for use as biodegradable materials within bone, Biomaterials, 29(10), 1329-44.
- [5].Jiang, Q.C., Wang, H.Y., Ma, B.X., Wang, Y. and Zhao, F. 2005. Fabrication of B<sub>4</sub>C Particulate reinforced Mg Matrix Composite by powder metallurgy, J. Alloy Compounds, 386(1-2), 177-181.
- [6] Schmid-Fetzer, R. and Grobner, J. 2001. Focused Development of Magnesium Alloys Using the Calphad Approach, Adv. Eng. Mater., 3(12), 947-961.
- [7] Housh, S., Mikucki, B. and Stevenson, A. 1990. Selection and Application of Magnesium and Magnesium Alloys, MetalsHandbook, 10th ed., ASM international, 2, 455-479.

- [8] Raynor, G.V. 1959. *The Physical Metallurgy of Magnesium and Its Alloys*, Pergamum Press, New York.
- [9] Morris, J.R., Ho, K.M., Chen, K.Y., Rengarajan, G. and Yoo, M.H. 2000. Large-scale atomistic study of core structures and energetic of &(( )); dislocations in hexagonal close packed metals, *Modelling and Simulation in Materials Science and Engineering*, 8(1), 25–35.
- [10] Enss, J., Everetz, T., Reier, T. and Juchmann, P. 2000. *Magnesium Alloys and their Applications*, in: K.U. Kainer (Ed.), Wiley–VCH, Munich, Germany (DGM, Weinheim).
- [11] Krajewski, P. 2001. Elevated Temperature Forming of Sheet Magnesium Alloys, SAE Paper, Warrendale, PA, SAE.
- [12] Siegert, K. and Jaeger, S. 2004. Pneumatic Bulging of Magnesium AZ31 Sheet Metal at Elevated Temperatures, *Magnesium Technology*, Alan Luo (TMS, Warrendale, PA), 87–90.
- [13] Jackson, J.H., Frost, P.D., Loonam, A.C., Eastwood, L.W. and Lorig, C.H. 1949. Magnesium-Lithium base alloys–preparation, fabrication and general characteristics, *metallurgical transactions*, 182, 149–168.
- [14] Busk, R.S., Leman, D.L. and Casey, J.J. 1950. The Properties of Some Magnesium-Lithium Alloys Containing Aluminum and Zinc, *J. Metals*, 188, 945–951.
- [15] Frost, ED., Kura, J.G. and Eastwood, L.W. 1950. Aging Characteristics of Magnesium-Lithium Base Alloys, *Trans. AIME*, 188, 1277–1282.
- [16] Schroth, J.G. 2004. General motors' quick plastic forming process, *Advances in Super plasticity and Super plastic Forming*, TMS warrendale, 9–20.
- [17] Murray, J. L. 1982. The Al-Mg (Aluminum-Magnesium) system, *Bulletin of Alloy Phase Diagrams*, 3(1), 60–74.
- [18] Tong, W., H. Tao, X. Jiang, N. Zhang, M. Marya, L.G. Hector, X.Q. Gayden, *Metall. Mater. Trans.* 36A (2005) 2651–2669.
- [18] Tong, W., Tao, H., Jiang, X., Zhang, N., Marya, M., Hector, L.G. and Gayden, X.Q. 2005. Deformation and fracture of miniature tensile bars with resistance spot-weld microstructures, *Metall. Mater. Trans.*, 36A, 2651-2669.
- [19] Tong, W., Tao, H., Zhang, N. and Hector, L.G. 2005. Time-resolved strain mapping measurements of individual Portevin-Le Chatelier deformation bands, *Scr. Mater.*, 53, 87-92.
- [20] Smith, B.W., Li, X. and Tong, W. 1998. Error assessment for strain mapping by digital image correlation, *Exp. Tech.*, 22 (4), 19-21.